direct effects of chemicals to the receptor-signal transduction systems. Our new assay, based on the hormone receptor mechanism, can rapidly screen a large number of the chemicals for their hormonal activities.

Since other hormone receptors employ similar mechanism as ER for the activation of the gene expression, it is possible to develop same assays for other hormone receptors. A newly developed ER assay is both reliable and efficient as a primary screening method of chemicals for estrogenic activities.

Acknowledgements

This work was supported by Ministry of Health, Labour and Welfare of Japan.

References

1. "*White paper on the endocrine disrupting chemicals '99* (Japanese)", Environmental Agency, Japan, **1999**.
2. M. Nakai, Y. Tabita, D. Asai, Y. Yakabe, T. Shinmyozu, M. Noguchi, M. Takatsuki, and Y. Shimohigashi, *Biochem. Biophys. Res. Commun.*, **1999**, *254*, 311.
3. "*The interim report by the committee on the effects on health by the endocrine disrupting chemicals* (Japanese)", Ministry of Health and Welfare, Japan, **1998**.
4. A. M. Soto and C. Sonnenschein, *Biochem. Biophys. Res. Commun.*, **1984**, *122*, 1097.
5. M. Pons, D. Gagne, J. C. Nicolas, and M. Mehtali, *BioTechniques*, **1990**, *9*, 450.
6. J. R. Reel, I. V. J. C. Lamb, and B. H. Neal, *Appl. Toxicol.*, **1996**, *34*, 288.
7. OECD, OECD VALIDATION WORK ON IN-VIVO UTEROPHIC SCREENING ASSAY, **1999**.
8. "*Methods of the Biological Assays of the Endocrine Disrupting Chemicals*", ed. T. Inoue, **2000**, Springer Verlag, Tokyo.
9. P. Diel, T. Schulz, K. M. molnikar, E. Trunck, G. Ollmer, and H. Ichna, *J. Steroid Biochem. Mol. Biol.*, **2000**, *73(1 - 2)*, 1.
10. "*Real-Time Analysis of Biomolecular Interactions*", ed. K. Nagata and H. Handa, **1998**, Springer Verlag, Tokyo.
11. B. J. Cheskis, S. Karathanasis, and C. R. Lyttle, *J. Biol. Chem.*, **1997**, 272, 11384.

Available online at www.sciencedirect.com
SCIENCE DIRECT®
ELSEVIER
Mutation Research 586 (2005) 1–17
Genetic Toxicology and Environmental Mutagenesis
www.elsevier.com/locate/gentox
Community address: www.elsevier.com/locate/mutres

Nitrogen-substitution effect on in vivo mutagenicity of chrysene

Katsuya Yamada [a], Takayoshi Suzuki [b,c], Arihiro Kohara [b], Taka-aki Kato [a], Makoto Hayashi [b], Takaharu Mizutani [a], Ken-ichi Saeki [a,*]

[a] *Graduate School of Pharmaceutical Sciences, Nagoya City University, Tanabedori, Mizuho-ku, Nagoya 467-8603, Japan*
[b] *Division of Genetics and Mutagenesis, National Institute of Health Sciences, 1-18-1 Kamiyoga, Setagaya-ku, Tokyo 158-8501, Japan*
[c] *Division of Cellular and Gene Therapy Products, National Institute of Health Sciences, 1-18-1 Kamiyoga, Setagaya-ku, Tokyo 158-8501, Japan*

Received 11 March 2005; received in revised form 28 April 2005; accepted 6 May 2005

Abstract

We have previously reported the in vivo mutagenicity of aza-polycyclic aromatic hydrocarbons (azaPAHs), such as quinoline, benzo[*f*]quinoline, benzo[*h*]quinoline, 1,7-phenanthroline and 10-azabenzo[*a*]pyrene. The 1,10-diazachrysene (1,10-DAC) and 4,10-DAC, nitrogen-substituted analogs of chrysene, were shown to exhibit mutagenicity in *Salmonella typhimurium* TA100 in the presence of rat liver S9 and human liver microsomes in our previous report, although DACs could not be converted to a bay-region diol epoxide, the ultimate active form of chrysene, because of their nitrogen atoms. In the present study, we tested in vivo mutagenicity of DACs compared with chrysene using the *lacZ* transgenic mouse (Muta™Mouse) to evaluate the effect of the nitrogen substitution. DACs- and chrysene-induced mutation in all of the six organs examined (liver, spleen, lung, kidney, bone marrow and colon). The mutant frequencies obtained with chrysene showed only small differences between the organs examined and ranged from 1.5 to 3 times the spontaneous frequency. The 4,10-DAC was more mutagenic than chrysene in all the organs tested. The highest *lacZ* mutation frequency was observed in the lung of 4,10-DAC-treated mice and it was 19 and 6 times the spontaneous frequency and the frequency induced by chrysene, respectively. The 1,10-DAC induced *lacZ* mutation in the lung with a frequency 4.3- and 1.5-fold higher than in the control and chrysene-treated mice, respectively, although the mutant frequencies in the other organs of 1,10-DAC-treated mice were almost equivalent to those of chrysene-treated mice. Not only chrysene but also DACs depressed the G:C to A:T transition and increased the G:C to T:A transversion in the liver and lung. These results suggest that the two types of nitrogen substitutions in the chrysene structure may enhance mutagenicity in the mouse lung, although they showed no difference in the target-organ specificity and the mutation spectrum.

Keywords: Aza-substitution; In vivo mutagenesis assay; Mutation spectrum

1. Introduction

We have been investigating the mutagenicity of aza-polycyclic aromatic hydrocarbons (azaPAHs) with

* Corresponding author. Tel.: +81 52 836 3485; fax: +81 52 834 9309.
E-mail address: saeki@phar.nagoya-cu.ac.jp (K. Saeki).

1383-5718/$ – see front matter © 2005 Elsevier B.V. All rights reserved.
doi:10.1016/j.mrgentox.2005.05.012

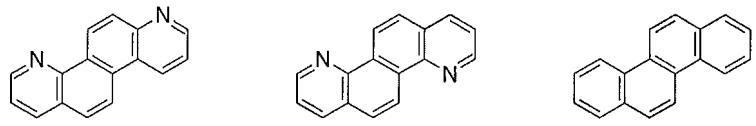

Fig. 1. Chemical structures of 1,10-DAC, 4,10-DAC and chrysene.

special attention to their metabolic activation mechanism. The 10-azabenzo[*a*]pyrene (10-azaBaP), a 10-aza-analog of benzo[*a*]pyrene (BaP), was reported to be as mutagenic as BaP in *Salmonella typhymurium* TA100 in the presence of PCB-treated rat liver S9 [1,2], although 10-azaBaP could not be converted to a bay-region diol epoxide, the ultimate mutagenic form of BaP [3,4], because of its nitrogen atom. We have previously reported that 10-azaBaP showed a higher mutagenicity than BaP in the Ames test using pooled human liver S9 [5]. However, in the in vivo mutagenesis assay system using the *lacZ* transgenic mouse (Muta^{TM}Mouse), 10-azaBaP was mutagenic only in the liver and colon and showed much less mutagenicity than BaP, which showed high mutagenicity in all of the organs tested [5]. Thus, 10-azaBaP interestingly showed differences in mutagenicity between the in vitro and in vivo assay systems.

We have also reported that quinoline, an aza-analog of naphthalene, one of simplest azaPAHs and a hepatocarcinogen [6,7], showed mutagenicity only in the liver of Muta^{TM}Mouse [8]. We also observed that it caused remarkable induction of G:C to C:G transversion [9] and suggested that it might be metabolically activated in the pyridine moiety to the ultimate mutagenic form [10]. Its active form was supposed to be an enamine epoxide (1,4-hydrated 2,3-epoxide), which would be responsible for the mutagenic modification of DNA [11–14]. Furthermore, three trycyclic azaPAHs, i.e., benzo[*f*]quinoline, benzo[*h*]quinoline and 1,7-phenanthroline, were shown to exhibit mutagenicity in Muta^{TM}Mouse in our previous report [15]. Benzo[*h*]quinoline and 1,7-phenanthroline were suggested to be converted to the ultimate genotoxic form in the pyridine moiety [16].

1,10-Diazachrysene (1,10-DAC) and 4,10-DAC are diaza-analogs of chrysene (Fig. 1), consisting of two quinoline moieties, and have structures similar to 10-azaBaP. We have previously reported that these DACs showed mutagenicity in Ames tests in the presence of rat liver S9 or human liver microsomes [17], although formation of the bay-region diol epoxide from DACs seemed impossible because of their nitrogen atoms. DACs have not been found in our living environments, but these are expected to be useful compounds to investigate the nature of mutagenicity in azaPAHs.

In the present study, we undertook to investigate the in vivo mutagenicity of DACs in comparison with chrysene by the in vivo mutation assay system using the *lacZ* transgenic mouse (Muta^{TM}Mouse) to evaluate the nitrogen-substitution effect in the chrysene skeleton on their mutagenicity.

2. Materials and methods

2.1. Materials

Chrysene (CAS Registry No. 218-01-9) and phenyl-β-D-galactoside (P-gal) were purchased from Sigma Chemical Co. (St. Louis, MO), proteinase K and olive oil from Wako Pure Chemicals (Osaka) and RNase from Boehringer Mannheim. The 1,10-DAC (CAS Registry No. 218-21-3) and 4,10-DAC (CAS Registry No. 218-34-8) were synthesized in this laboratory according to the reported methods [18].

2.2. In vivo mutagenesis assays using Muta^{TM}Mouse

2.2.1. Animals and treatments

Male Muta^{TM}Mice, at 7–8 weeks of age, were supplied by COVANCE Research Products (PA, USA) and acclimatized for 1 week before use. Chrysene and 4,10-DAC dissolved in olive oil (10 mL/kg body weight)

were injected intraperitoneally into four mice each at a single dose of 200 mg/kg once a week for 4 consecutive weeks (800 mg/kg in total). The 1,10-DAC dissolved in olive oil (10 mL/kg body weight) was injected into four mice at a single dose of 100 mg/kg similarly (400 mg/kg in total). Four control mice were given 10 mL olive oil/kg.

2.2.2. Tissues and DNA isolation

All mice were killed by cervical dislocation 7 days after the last administration of test chemicals. The liver, spleen, lung, kidney, bone marrow and colon were immediately extirpated, frozen in liquid nitrogen and stored at −80 °C until DNA extraction. The genomic DNA was extracted from each tissue by the phenol/chloroform method according to the Muta™Mouse/PS Mutation Assay Manual (Corning Hazleton, 1995). The isolated DNA, which was precipitated with ethanol, was air-dried and dissolved in an appropriate volume (20–200 μL) of TE-4 buffer (10 mM Tris–HCl at pH 8.0 containing 4 mM EDTA) at room temperature overnight. The DNA solution thus prepared was stored at 4 °C.

2.2.3. In vitro packaging

The lambda gt10/*lacZ* vector could be efficiently recovered by in vitro packaging reactions [19]. Our homemade packaging extract (HM) consisting of sonic extract (SE) of *Escherichia coli* NM759 and freeze–thaw lysate (FTL) of *E. coli* BHB2688 was prepared according to the method of Gunther et al. [20]. As a general procedure for handling the HM extract, approximately, 5 μg DNA was mixed with 15 μL of FTL and 30 μL of SE and incubated at 37 °C for 90 min. Then SE and FTL were added again and the mixture was incubated for another 90 min. The reaction was terminated by the addition of an appropriate volume of SM buffer (50 mM Tris–HCl at pH 7.5, 10 mM $MgSO_4$, 100 mM NaCl and 0.01% gelatin) and the mixture was stored at 4 °C. By this procedure, the lambda gt10 vector to form an infectious phage was efficiently rescued from genomic DNA.

2.2.4. Mutation assays

2.2.4.1. lacZ mutant frequency determination. The positive selection for *lacZ* mutants was performed as previously reported [21–23]. Briefly, the phage

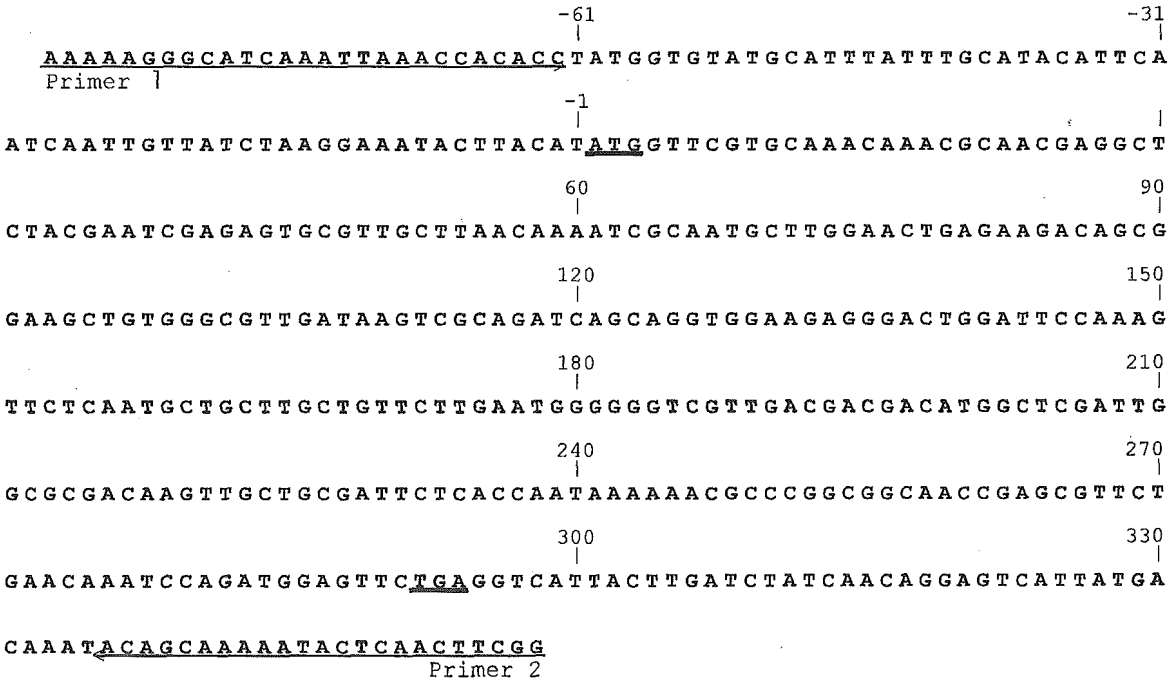

Fig. 2. Sequence map of the *cII* gene; primers used for PCR amplification and sequencing are shown by arrows. The PCR gives 446 bp products that involve the entire (294 bp) *cII* gene. Initiation and stop codons are underlined.

Table 1
Mutant frequencies induced by 1,10-DAC, 4,10-DAC and chrysene in six organs of Muta™Mouse

Tissue	Treatment	*lacZ* assay				*cII* assay			
		Individual animal data			Average ± S.D.	Individual animal data			Average ±S.D.
		No. of phages analyzed	No. of mutants	MF × 10^6	MF × 10^6	No. of phages analyzed	No. of mutants	MF × 10^6	MF × 10^6
Liver	Control (olive oil)	463000	36	77.8		1547000	31	20.0	
		173000	12	69.4		602000	20	33.2	
		1899000	247	130.1		1618000	47	29.0	
		396000	30	75.8	88.2 ± 24.3	1398000	22	15.7	24.5 ± 7.0
	1,10-DAC	391000	77	196.9		1299000	90	69.3	
		1126000	127	112.8		989000	40	40.4	
		371500	63	169.6		1805000	72	39.9	
		244000	36	147.5	156.7 ± 30.8*	1095000	23	21.0	42.7 ± 17.3
	4,10-DAC	192000	72	375.0		731000	79	108.1	
		355500	193	542.9		1446000	182	125.9	
		506500	225	444.2		2080000	233	112.0	
		503000	308	612.3	493.6 ± 90.9**	1751000	311	177.6	130.9 ± 27.8**
	Chrysene	452500	98	216.6		1025000	51	49.8	
		322500	88	272.9		1220000	81	66.4	
		362500	88	242.8		1343000	68	50.6	
		522000	89	170.5	225.7 ± 37.6**	1799000	60	33.4	50.0 ± 11.7*
Spleen	Control (olive oil)	866000	47	54.3		966000	14	14.5	
		1145000	59	51.5		1180000	25	21.2	
		870000	36	41.4		1024000	34	33.2	
		653500	23	35.2	45.6 ± 7.7	1039000	15	14.4	20.8 ± 7.7
	1,10-DAC	1700500	150	88.2		1550000	70	45.2	
		769000	77	100.1		909000	59	64.9	
		1252000	125	99.8		2119000	129	60.9	
		1316000	131	99.5	96.9 ± 5.0**	1837000	110	59.9	57.7 ± 7.5**
	4,10-DAC	469500	109	232.2		550000	56	101.8	
		1506000	525	348.6		1754000	260	148.2	
		1410000	374	265.2		2071000	268	129.4	
		1115000	271	243.0	272.3 ± 45.7**	1438000	219	152.3	132.9 ± 19.9**
	Chrysene	2225000	339	152.4		470500	12	25.5	
		638000	66	103.4		970000	72	74.2	
		1433500	202	140.9		2313000	102	44.1	
		247500	34	137.4	133.5 ± 18.2**	612000	13	21.2	41.3 ± 20.9
Lung	Control (olive oil)	310000	10	32.3		376000	14	37.2	
		296500	28	94.4		263500	11	41.7	
		646000	63	97.5		2016000	73	36.2	
		1402000	73	52.1	69.1 ± 27.8	1429000	23	16.1	32.8 ± 9.9
	1,10-DAC	1911000	539	282.1		1855000	255	137.5	
		1691000	342	202.2		1921000	151	78.6	
		1242000	430	346.2		1807000	183	101.3	
		1826500	652	357.0	296.9 ± 61.7**	2152000	281	130.6	112.0 ± 23.6**
	4,10-DAC	979500	1402	1431.3		1112000	530	476.6	
		1489000	1659	1114.2		1747000	771	441.3	
		1497000	2343	1565.1		1900000	1093	575.3	

Table 1 (*Continued*)

Tissue	Treatment	*lacZ* assay				*cII* assay			
		Individual animal data			Average ± S.D.	Individual animal data			Average ±S.D.
		No. of phages analyzed	No. of mutants	MF × 10^6	MF × 10^6	No. of phages analyzed	No. of mutants	MF × 10^6	MF × 10^6
		1673000	1702	1017.3	1282.0 ± 224.0**	1847000	1005	544.1	509.3 ± 53.0**
	Chrysene	1033000	121	117.1		1577000	61	38.7	
		1526000	371	243.1		2067000	231	111.8	
		1101000	241	218.9		1566000	115	73.4	
		871000	177	203.2	195.6 ± 47.5**	1254000	69	55.0	69.7 ± 27.2
Kidney	Control (olive oil)	447000	36	80.5		546000	21	38.5	
		741500	61	82.3		925000	23	24.9	
		1726000	62	35.9		2183000	70	32.1	
		1948000	72	37.0	58.9 ± 22.5	2244000	57	25.4	30.2 ± 5.6
	1,10-DAC	1609000	214	133.0		2570000	109	42.4	
		1510000	138	91.4		2278000	127	55.8	
		1410000	114	80.9		2621000	96	36.6	
		945000	119	125.9	107.8 ± 22.1*	1658000	67	40.4	43.8 ± 7.2*
	4,10-DAC	1378000	175	127.0		1695500	115	67.8	
		2101000	412	196.1		2526000	270	106.9	
		1447000	235	162.4		2217000	153	69.0	
		1355000	402	296.7	195.5 ± 63.3*	2014000	232	115.2	89.7 ± 21.5**
	Chrysene	1177000	161	136.8		2304000	101	43.8	
		1583000	239	151.0		2415000	157	65.0	
		1187500	241	202.9		2224000	115	51.7	
		1785000	257	144.0	158.7 ± 26.0**	2968000	147	49.5	52.5 ± 7.8**
Bone marrow	Control (olive oil)	421000	20	47.5		580000	12	20.7	
		1034000	48	46.4		1094000	25	22.9	
		1080000	61	56.5		1202000	38	31.6	
		1352000	48	35.5	46.5 ± 7.4	906000	17	18.8	23.5 ± 4.9
	1,10-DAC	1131000	78	69.0		1406000	57	40.5	
		764500	86	112.5		916000	39	42.6	
		1209000	108	89.3		1525000	58	38.0	
		732000	72	98.4	92.3 ± 15.8**	858000	48	55.9	44.3 ± 6.9**
	4,10-DAC	503500	147	292.0		779000	90	115.5	
		621000	239	384.9		1074000	191	177.8	
		1010000	200	198.0		1075000	104	96.7	
		829000	196	236.4	277.8 ± 70.2*	945000	124	131.2	130.3 ± 30.0**
	Chrysene	757500	65	85.8		1179000	20	17.0	
		819000	55	67.2		1046000	46	44.0	
		799500	49	61.3		1331000	33	24.8	
		853500	60	70.3	71.1 ± 9.1*	1392000	25	18.0	25.9 ± 10.9
Colon	Control (olive oil)	369500	17	46.0		1058000	43	40.6	
		1064000	77	72.4		1052000	40	38.0	
		660000	63	95.5		840000	36	42.9	
		676000	55	81.4	73.8 ± 18.0	1187000	33	27.8	37.3 ± 5.8
	1,10-DAC	306500	41	133.8		1715000	85	49.6	
		207000	25	120.8		1250000	57	45.6	

Table 1 (*Continued*)

Tissue	Treatment	*lacZ* assay				*cII* assay			
		Individual animal data			Average ± S.D.	Individual animal data			Average ±S.D.
		No. of phages analyzed	No. of mutants	MF × 10^6	MF × 10^6	No. of phages analyzed	No. of mutants	MF × 10^6	MF × 10^6
		988000	91	92.1		1396000	74	53.0	
		577000	75	130.0	119.2 ± 16.3*	951000	62	65.2	53.3 ± 7.3*
	4,10-DAC	469000	42	89.6		734000	48	65.4	
		369500	211	571.0		1425000	292	204.9	
		1004000	245	244.0		1089000	152	139.6	
		395000	188	475.9	345.1 ± 189.5	954000	187	196.0	151.5 ± 55.7*
	Chrysene	266500	29	108.8		980000	44	44.9	
		379000	52	137.2		1034000	68	65.8	
		1223000	222	181.5		1612000	78	48.4	
		615000	93	151.2	144.7 ± 26.2**	1178000	44	37.4	49.1 ± 10.4

Significantly different from the control group.
* $P<0.05$.
** $P<0.01$.

solution was absorbed to *E. coli* C (*lac*$^-$ *galE*$^-$) at room temperature for 20–30 min. For titration, appropriately diluted phage–*E. coli* solution was mixed with LB top agar (containing 10 mM $MgSO_4$) and plated onto dishes containing bottom agar. The remaining phage–*E. coli* solution was mixed with LB top agar containing phenyl-β-D-galactoside (3 mg/mL) and plated as described above. The mutant frequency (MF) was calculated by the following formula:

mutant frequency = (total number of plaques on selection plates/total number of plaques on titer plates) × dilution factor.

The significance of differences in the mutant frequency between the treated and control groups was analyzed by using Student's *t*-test and Welch's *t*-test in combination with the *F*-test.

2.2.4.2. cII mutant frequency determination. In the present study, we examined the mutagenicity in the lambda *cII* gene, which is also integrated as a lambda vector gene, which serves as another selective marker as reported previously in the *lacI* transgenic BigBlue mouse [24]. The positive selection for *cII* mutants was performed according to the method of Jakubczak et al. [24] with a slight modification as previously reported [9]. Briefly, the phage solution was absorbed to *E. coli* G1225 (*hfl*$^-$) at room temperature for 20–30 min. For titration, appropriately diluted phage–*E. coli* solution was mixed with LB top agar (containing 10 mM $MgSO_4$) and plated onto dishes containing bottom agar and the plates were incubated at 37 °C for 24 h. The remaining phage–*E. coli* solution was mixed with LB top agar and plated onto dishes containing bottom agar. The plates were incubated at 25 °C for 48 h for selection of *cII* mutants. The wild-type phage, recovered from Muta^{TM}Mice, has a *cI*$^-$ phenotype, which permits plaque formation with the *hfl*$^-$ strain at 37 °C but not at 25 °C. The mutant frequency was calculated by the following formula:

mutant frequency = (total number of plaques on selection plates/total number of plaques on titer plates) × dilution factor.

The significance of differences in the mutant frequency between the treated and control groups was analyzed by using Student's *t*-test and Welch's *t*-test in combination with the *F*-test.

2.2.5. Sequencing of mutants

The entire lambda *cII* region was amplified directly from mutant plaques by Taq DNA polymerase (Takara Shuzo, Tokyo, Japan) with primers P1, 5′-AAAAAGGGCATCAAATTAAACC-3′ and P2, 5′-CCGAAGTTGAGTATTTTTGCTGT-3′ as previously reported [9] (Fig. 2). A 446 bp PCR product was puri-

fied with a microspin column (Amersham Pharmacia, Tokyo, Japan) and then used for a sequencing reaction with the Ampli Taq cycle sequencing kit (PE Biosystems, Tokyo, Japan) using the primer P1. The reaction product was isolated by ethanol precipitation and analyzed with the ABI PRISM™ 310 genetic analyzer (PE Biosystems). In this study, about 40 mutants were subjected to sequence analysis in each group both in the liver and lung.

3. Results

3.1. Mutant frequencies by 1,10-DAC, 4,10-DAC and chrysene

Chrysene and its diaza-analogs, 1,10-DAC and 4,10-DAC, were tested for in vivo mutagenicity using *lacZ* transgenic mice (Muta™Mice). Chrysene and 4,10-DAC were injected at the total dose of 800 mg/kg

Table 2
Sequences of *cII* mutations in the liver of 1,10-DAC-treated Muta™Mouse

Mutant no.	Position	Mutation	Sequence			Amino acid change
C1	117	G to T	TCG	CAG	ATC	Gln to His
C2	42	G to T	ATC	GAG	AGT	Glu to Asp
C3	126	G to T	AGC	AGG	TGG	Arg to Ser
C4	40–43	−GA	GAG	AGT	GCG	Frameshift
C5	166	G to T	CTT	GCT	GTT	Ala to Ser
C6	233	T to A	ATT	CTC	ACC	Leu to His
C7	132	G to T	TGG	AAG	AGG	Lys to Asn
C8	89	C to T	ACA	GCG	GAA	Ala to Val
C9	11	C to TA	CGT	GCA	AAC	Frameshift
C10	178	T to A	GAA	TGG	GGG	Trp to Arg
C11	197	A to G	GAC	GAC	ATG	Asp to Gly
C12	179	G to T	GAA	TGG	GGG	Trp to Leu
C13	29	C to A	GAG	GCT	CTA	Ala to Asp
C14	101	G to T	GTG	GGC	GTT	Gly to Val
C15	89	C to T	ACA	GCG	GAA	Ala to Val
C16	117	G to C	TCG	CAG	ATC	Gln to His
C17	40	G to A	ATC	GAG	AGT	Glu to Lys
C18	294	A to C	TTC	TGA	–	Stop to Cys
C19	150	G to T	CCA	AAG	TTC	Lys to Asn
C20[a]	294	A to C	TTC	TGA	–	Stop to Cys
C21	211	G to A	TTG	GCG	CGA	Ala to Thr
C22	111	G to T	GAT	AAG	TCG	Lys to Asn
C23	123	C to A	ATC	AGC	AGG	Ser to Arg
C24	160	C to A	ATG	CTG	CTT	Leu to Met
C25	173	T to C	GTT	CTT	GAA	Leu to Pro
C26	125	G to C	AGC	AGG	TGG	Arg to Thr
C27	−3	C to G	tta	cat	ATG	Base substitution in the 5′-flanking region
C28	29	C to A	GAG	GCT	CTA	Ala to Asp
C29[a]	111	G to T	GAT	AAG	TCG	Lys to Asn
C30	38	T to A	CGA	ATC	GAG	Ile to Asn
C31	40	G to T	ATC	GAG	AGT	Glu to Stop
C32	163	C to T	CTG	CTT	GCT	Leu to Phe
C33	79	G to T	ACT	GAG	AAG	Glu to Stop
C34	57	C to A	CTT	AAC	AAA	Asn to Lys
C35	89	C to T	ACA	GCG	GAA	Ala to Val
C36	179–184	−G	TGG	GGG	GTC	Frameshift
C37	113	C to A	AAG	TCG	CAG	Ser to Stop
C38	89	C to G	ACA	GCG	GAA	Ala to Gly
C39	123	C to G	ATC	AGC	AGG	Ser to Arg
C40	125	G to A	AGC	AGG	TGG	Arg to Lys

[a] Ascribable to the same mutation obtained in an identical mouse.

intraperitoneally, based on the tolerance dose. The total dose of 1,10-DAC was 400 mg/kg because 1,10-DAC showed more toxicity than 4,10-DAC and chrysene in a preliminary test. The mutant frequencies observed with the DNA preparations extracted from the six organs at 7 days after the last injection are shown in Table 1. More than 10 mutant plaques were analyzed in all organs.

The spontaneous mutant frequencies observed in the control group were similar among the six organs in both *lacZ* and *cII* assays, in the rate ranges of 46×10^{-6} to 88×10^{-6} and 21×10^{-6} to 37×10^{-6}, respectively. These results were comparable to our previous studies [5,8–10,15,25].

All the test compounds significantly increased the mutant frequencies in all the tested organs in the *lacZ*

Table 3
Sequences of *cII* mutations in the liver of 4,10-DAC-treated Muta™Mouse

Mutant no.	Position	Mutation	Sequence			Amino acid change
D1	113	C to T	AAG	TCG	CAG	Ser to Leu
D2	86	C to A	AAG	ACA	GCG	Thr to Lys
D3	65	C to A	ATC	GCA	ATG	Ala to Glu
D4	106	G to T	GTT	GAT	AAG	Asp to Tyr
D5	101	G to T	GTG	GGC	GTT	Gly to Val
D6	101	G to C	GTG	GGC	GTT	Gly to Ala
D7	29–30	CT to TC	GAG	GCT	CTA	Ala to Val
D8	74	G to T	CTT	GGA	ACT	Gly to Val
D9	115	C to A	TCG	CAG	ATC	Gln to Lys
D10[a]	113	C to T	AAG	TCG	CAG	Ser to Leu
D11	42	G to T	ATC	GAG	AGT	Glu to Asp
D12	119	T to A	CAG	ATC	AGC	Ile to Asn
D13	150	G to T	CCA	AAG	TTC	Lys to Asn
D14	190	G to T	GTT	GAC	GAC	Asp to Tyr
D15	103	G to T	GGC	GTT	GAT	Val to Phe
D16	106	G to T	GTT	GAT	AAG	Asp to Tyr
D17	101	G to A	GTG	GGC	GTT	Gly to Asp
D18	196	G to A	GAC	GAC	ATG	Asp to Asn
D19	226	G to C	GCT	GCG	ATT	Ala to Pro
D20	214	C to T	GCG	CGA	CAA	Arg to Stop
D21	47	C to G	AGT	GCG	TTG	Ala to Gly
D22	91	G to T	GCG	GAA	GCT	Glu to Stop
D23	86	C to G	AAG	ACA	GCG	Thr to Arg
D24	132	G to T	TGG	AAG	AGG	Lys to Asn
D25	123	C to A	ATC	AGC	AGG	Ser to Arg
D26	196	G to C	GAC	GAC	ATG	Asp to His
D27	52	C to T	TTG	CTT	AAC	Leu to Phe
D28	64	G to C	ATC	GCA	ATG	Ala to Pro
D29	163	C to T	CTG	CTT	GCT	Leu to Phe
D30[a]	132	G to T	TGG	AAG	AGG	Lys to Asn
D31	125	G to A	AGC	AGG	TGG	Arg to Lys
D32	196	G to A	GAC	GAC	ATG	Asp to Asn
D33	179–184	−G	TGG	GGG	GTC	Frameshift
D34	148	A to C	CCA	AAG	TTC	Lys to Gln
D35	117	G to T	TCG	CAG	ATC	Gln to His
D36	141	G to T	GAC	TGG	ATT	Trp to Cys
D37	103	G to T	GGC	GTT	GAT	Val to Phe
D38	160	C to A	ATG	CTG	CTT	Leu to Met
D39	125–126	GG to TT	AGC	AGG	TGG	Arg to Ile
D40	166	G to C	CTT	GCT	GTT	Ala to Pro

[a] Ascribable to the same mutation obtained in an identical mouse.

assay and/or *cII* assay. The 4,10-DAC showed the highest mutagenicity among the test compounds, and the highest *lacZ* mutant frequency of 4,10-DAC, observed in the lung, was 19-, 6- and 4-fold over the spontaneously, chrysene- and 1,10-DAC-induced frequencies, respectively. The highest *lacZ* mutant frequency of 1,10-DAC was also observed in the lung. Mutant frequencies obtained with chrysene were not different between the organs examined and ranged from 1.5- to 3-fold over the spontaneous frequency. The mutant frequencies in the *cII* assay showed a tendency similar to those in the *lacZ* assay.

3.2. Mutation spectra of DACs and chrysene in the liver and lung

Thirty-six and 38 control mutants in the liver and lung, respectively, were subjected to sequence analysis, together with 37 and 39 chrysene-induced mutants, 40 and 43 induced mutants of 1,10-DAC and 40

Table 4
Sequences of *cII* mutations in the liver of chrysene-treated Muta™Mouse

Mutant no.	Position	Mutation	Sequence			Amino acid change
B1	210	G to T	CGA	TTG	GCG	Leu to Phe
B2	214	C to T	GCG	CGA	CAA	Arg to Stop
B3	107	A to G	GTT	GAT	AAG	Asp to Gly
B4	150	G to T	CCA	AAG	TTC	Lys to Asn
B5	113	C to T	AAG	TCG	CAG	Ser to Leu
B6	220	G to T	CAA	GTT	GCT	Val to Phe
B7	132	G to T	TGG	AAG	AGG	Lys to Asn
B8	34	C to T	CTA	CGA	ATC	Arg to Stop
B9	40	G to A	ATC	GAG	AGT	Glu to Lys
B10	272–273	−A	TCT	GAA	CAA	Frameshift
B11	190–198	−GAC	GAC	GAC	GAC	Deletion
B12	107	A to G	GTT	GAT	AAG	Asp to Gly
B13	42	G to T	ATC	GAG	AGT	Glu to Asp
B14	125	G to T	AGC	AGG	TGG	Arg to Met
B15	57	C to A	CTT	AAC	AAA	Asn to Lys
B16	141	G to C	GAC	TGG	ATT	Trp to Cys
B17[a]	190–198	−GAC	GAC	GAC	GAC	Frameshift
B18	74	G to A	CTT	GGA	ACT	Gly to Glu
B19	86	C to G	AAG	ACA	GCG	Thr to Arg
B20	196	G to C	GAC	GAC	ATG	Asp to His
B21	91	G to T	GCG	GAA	GCT	Glu to Stop
B22	178	T to G	GAA	TGG	GGG	Trp to Gly
B23	212	C to A	TTG	GCG	CGA	Ala to Glu
B24	127	T to A	AGG	TGG	AAG	Trp to Arg
B25	88	G to C	ACA	GCG	GAA	Ala to Pro
B26	196	G to A	GAC	GAC	ATG	Asp to Asn
B27	129	G to T	AGG	TGG	AAG	Trp to Cys
B28	88	G to A	ACA	GCG	GAA	Ala to Thr
B29	99–101	−G	GTG	GGC	GTT	Frameshift
B30	212	C to A	TTG	GCG	CGA	Ala to Glu
B31	124	A to T	AGC	AGG	TGG	Arg to Trp
B32	179–184	−G	TGG	GGG	GTC	Frameshift
B33	91	G to T	GCG	GAA	GCT	Glu to Stop
B34	101	G to A	GTG	GGC	GTT	Gly to Asp
B35	89	C to T	ACA	GCG	GAA	Ala to Val
B36	89	C to A	ACA	GCG	GAA	Ala to Glu
B37	163	C to G	CTG	CTT	GCT	Leu to Val

[a] Ascribable to the same mutation obtained in an identical mouse.

Table 5
Sequences of *cII* mutations in the liver of control Muta™Mouse

Mutant no.	Position	Mutation	Sequence			Amino acid change
A1	40	G to A	ATC	GAG	AGT	Glu to Lys
A2	205–213	−CGATTGGCG				Deletion
A3	34	C to T	CTA	CGA	ATC	Arg to Stop
A4	115	C to A	TCG	CAG	ATC	Gln to Lys
A5	212	C to T	TTG	GCG	CGA	Ala to Val
A6	89	C to A	ACA	GCG	GAA	Ala to Glu
A7	119–208	−ATGGCTCGAT				Deletion
A8	122	G to T	ATC	AGC	AGG	Ser to Ile
A9	233	T to C	ATT	CTC	ACC	Leu to Pro
A10	212	C to T	TTG	GCG	CGA	Ala to Val
A11[a]	89	C to A	ACA	GCG	GAA	Ala to Glu
A12	150	G to T	CCA	AAG	TTC	Lys to Asn
A13	205	C to T	GCT	CGA	TTG	Arg to Stop
A14	95	C to A	GAA	GCT	GTG	Ala to Asp
A15	89	C to T	ACA	GCG	GAA	Ala to Val
A16	212	C to T	TTG	GCG	CGA	Ala to Val
A17	122	G to T	ATC	AGC	AGG	Ser to Ile
A18[a]	150	G to T	CCA	AAG	TTC	Lys to Asn
A19	113	C to T	AAG	TCG	CAG	Ser to Leu
A20	210	G to T	CGA	TTG	GCG	Leu to Phe
A21	212	C to T	TTG	GCG	CGA	Ala to Val
A22	34	C to T	CTA	CGA	ATC	Arg to Stop
A23	110	A to T	GAT	AAG	TCG	Lys to Met
A24	241–246	−A	AAA	AAA	CGC	Frameshift
A25	196	G to A	GAC	GAC	ATG	Asp to Asn
A26[a]	34	C to T	CTA	CGA	ATC	Arg to Stop
A27	107	A to C	GTT	GAT	AAG	Asp to Ala
A28	89	C to T	ACA	GCG	GAA	Ala to Val
A29	196	G to A	GAC	GAC	ATG	Asp to Asn
A30	212	C to T	TTG	GCG	CGA	Ala to Val
A31	3	G to A	–	ATG	GTT	Met to Ile
A32	179–184	−G	TGG	GGG	GTC	Frameshift
A33	95	C to G	GAA	GCT	GTG	Ala to Gly
A34	110	A to C	GAT	AAG	TCG	Lys to Thr
A35[a]	89	C to T	ACA	GCG	GAA	Ala to Val
A36[a]	110	A to C	GAT	AAG	TCG	Lys to Thr

[a] Ascribable to the same mutation obtained in an identical mouse.

and 42 induced mutants of 4,10-DAC in the respective two organs. The mutations are characterized in Tables 2–9 and summarized in Tables 10 and 11. In Tables 10 and 11, the same mutations from an identical mouse were treated as a single event.

In the liver, spontaneous mutations consisted mainly of G:C to A:T transitions (14/30) followed by G:C to T:A transversions (7/30) as shown in the previous report on the *cII* mutant spectrum in the liver of control Muta™Mouse [9,26].

The majority of chrysene-induced mutations were G:C to T:A transversions (13/36), followed by the G:C to A:T transitions (9/36). Both 1,10-DAC- and 4,10-DAC-induced mutations also consisted mainly of G:C to T:A transversions (17/38 and 18/38, respectively). The *cII* mutant spectra by all the test compounds in the lung showed a tendency similar to those in the liver.

4. Discussion

1,10-DAC and 4,10-DAC, the tetracyclic azaPAHs and diaza-analogs of chrysene, could not be converted to the bay-region diol epoxide form because of their nitrogen atoms in the benzene rings of the bay-region

Table 6
Sequences of *cII* mutations in the lung of 1,10-DAC-treated Muta™Mouse

Mutant no.	Position	Mutation	Sequence			Amino acid change
c1	163–164	CT to AA	CTG	CTT	GCT	Leu to Asn
c2	215	G to C	GCG	CGA	CAA	Arg to Pro
c3	132	G to T	TGG	AAG	AGG	Lys to Asn
c4	79	G to T	ACT	GAG	AAG	Glu to Stop
c5	160–161	CT to AG	ATG	CTG	CTT	Leu to Arg
c6	178	T to A	ATG	CTG	CTT	Trp to Arg
c7	100–101	GG to AT	GTG	GGC	GTT	Gly to Ile
c8	65	C to A	ATC	GCA	ATG	Ala to Glu
c9	150	G to T	CCA	AAG	TTC	Lys to Asn
c10[a]	79	G to T	ACT	GAG	AAG	Glu to Stop
c11	132	G to T	TGG	AAG	AGG	Lys to Asn
c12	34	C to T	CTA	CGA	ATC	Arg to Stop
c13	140	G to C	GAC	TGG	ATT	Trp to Ser
c14	179–184	–G	TGG	GGG	GTC	Frameshift
c15	212	C to T	TTG	GCG	CGA	Ala to Val
c16	141	G to T	GAC	TGG	ATT	Trp to Cys
c17	62	T to C	AAA	ATC	GCA	Ile to Thr
c18	196	G to T	GAC	GAC	ATG	Asp to Tyr
c19	212	C to G	TTG	GCG	CGA	Ala to Gly
c20	42	G to T	ATC	GAG	AGT	Glu to Asp
c21	160	C to A	ATG	CTG	CTT	Leu to Met
c22	215	G to C	GCG	CGA	CAA	Arg to Pro
c23	127	T to G	AGG	TGG	AAG	Trp to Gly
c24	64	G to T	ATC	GCA	ATG	Ala to Ser
c25	100	G to A	GTG	GGC	GTT	Gly to Ser
c26	111	G to T	GAT	AAG	TCG	Lys to Asn
c27	62	T to G	AAA	ATC	GCA	Ile to Ser
c28	196	G to T	GAC	GAC	ATG	Asp to Tyr
c29	179–184	–G	TGG	GGG	GTC	Frameshift
c30	122	G to T	ATC	AGC	AGG	Ser to Ile
c31	126	G to C	AGC	AGG	TGG	Arg to Ser
c32	128	G to T	AGG	TGG	AAG	Trp to Leu
c33	161	T to A	ATG	CTG	CTT	Leu to Gln
c34	129	G to T	AGG	TGG	AAG	Trp to Cys
c35	179–184	–G	TGG	GGG	GTC	Frameshift
c36	164–165	–T	CTG	CTT	GCT	Frameshift
c37	150	G to T	CCA	AAG	TTC	Lys to Asn
c38	178	T to G	GAA	TGG	GGG	Trp to Gly
c39	167	C to G	CTT	GCT	GTT	Ala to Gly
c40	106	G to T	GTT	GAT	AAG	Asp to Tyr
c41	51	G to C	GCG	TTG	CTT	Leu to Phe
c42	133	A to T	AAG	AGG	GAC	Arg to Trp
c43	169	G to C	GCT	GTT	CTT	Val to Leu

[a] Ascribable to the same mutation obtained in an identical mouse.

epoxide or diol moiety. Nevertheless, 1,10-DAC and 4,10-DAC showed in vitro mutagenicity in the Ames tests using rat liver S9 or human liver microsomes in our previous study [17]. Therefore, these DACs might be converted to ultimate mutagenic forms by a mechanism different from that of chrysene. We have investigated the in vivo mutagenicity of some aza-PAHs, such as quinoline and 10-azaBaP [5,8–10,15]. The 1,10-DAC and 4,10-DAC consist of two quinoline moieties and also have a structure similar to 10-azaBaP. In the present study, we attempted to investigate the in vivo mutagenicity of DACs compared with chrysene

Table 7
Sequences of *cII* mutations in the lung of 4,10-DAC-treated Muta™Mouse

Mutant no.	Position	Mutation	Sequence			Amino acid change
d1	123	C to A	ATC	AGC	AGG	Ser to Arg
	138	C to A	AGG	GAC	TGG	Asp to Glu
d2	29	C to A	GAG	GCT	CTA	Ala to Asp
d3	117	G to T	TCG	CAG	ATC	Gln to His
d4	212	C to T	TTG	GCG	CGA	Ala to Val
d5	125	G to T	AGC	AGG	TGG	Arg to Met
d6	160	C to A	ATG	CTG	CTT	Leu to Met
d7	128	G to T	AGG	TGG	AAG	Trp to Leu
d8	293	G to T	TTC	TGA	–	Stop to Leu
d9	220	G to T	CAA	GTT	GCT	Val to Phe
d10	57	C to A	CTT	AAC	AAA	Asn to Lys
d11	111	G to T	GAT	AAG	TCG	Lys to Asn
d12	115	C to A	TCG	CAG	ATC	Gln to Lys
d13	51	G to T	GCG	TTG	CTT	Leu to Phe
d14	179–184	−G	TGG	GGG	GTC	Frameshift
d15	115	C to T	TCG	CAG	ATC	Gln to Stop
d16	88	G to C	ACA	GCG	GAA	Ala to Pro
d17	132	G to T	TGG	AAG	AGG	Lys to Asn
d18	117	G to T	TCG	CAG	ATC	Gln to His
d19	65	C to A	ATC	GCA	ATG	Ala to Glu
d20[a]	115	C to A	TCG	CAG	ATC	Gln to Lys
d21[a]	88	G to C	ACA	GCG	GAA	Ala to Pro
d22	145	C to G	ATT	CCA	AAG	Pro to Ala
d23	103	G to T	GGC	GTT	GAT	Val to Phe
d24	167	C to G	CTT	GCT	GTT	Ala to Gly
d25	212	C to G	TTG	GCG	CGA	Ala to Gly
d26	163	C to T	CTG	CTT	GCT	Leu to Phe
d27	224	C to A	GTT	GCT	GCG	Ala to Asp
d28	175	G to T	CTT	GAA	TGG	Glu to Stop
d29	40	G to A	ATC	GAG	AGT	Glu to Lys
d30	160	C to A	ATG	CTG	CTT	Leu to Met
d31[a]	103	G to T	GGC	GTT	GAT	Val to Phe
d32	89	C to T	ACA	GCG	GAA	Ala to Val
d33	179–184	−G	TGG	GGG	GTC	Frameshift
d34	95	C to A	GAA	GCT	GTG	Ala to Asp
d35	134	G to T	AAG	AGG	GAC	Arg to Met
d36	101	G to T	GTG	GGC	GTT	Gly to Val
d37	34	C to T	CTA	CGA	ATC	Arg to Stop
d38	129	G to T	AGG	TGG	AAG	Trp to Cys
d39	89	−C	ACA	GCG	GAA	Frameshift
d40	125	G to T	AGC	AGG	TGG	Arg to Met
d41	65	C to A	ATC	GCA	ATG	Ala to Glu
d42	122	G to T	ATC	AGC	AGG	Ser to Ile

[a] Ascribable to the same mutation obtained in an identical mouse.

to understand the nature of the in vivo mutagenicity of azaPAHs.

Table 12 summarizes the in vivo mutagenicity of a series of azaPAHs with the pyridine moiety, investigated in our previous and present studies using Muta™Mouse. One of the authors (T.S.) reported that the median toxic dose (TD_{50}) of chemicals as used for numerical description of their carcinogenic potency is well correlated with in vivo mutagenic potency, which was calculated by division of the chemical-induced mutant frequency by the total injection dose of the chemical in the transgenic mouse [27]. We calculated

Table 8
Sequences of *cII* mutations in the lung of chrysene-treated Muta™Mouse

Mutant no.	Position	Mutation	Sequence			Amino acid change
b1	112	T to C	AAG	TCG	CAG	Ser to Pro
b2	89	C to T	ACA	GCG	GAA	Ala to Val
b3	34	C to T	CTA	CGA	ATC	Arg to Stop
b4	141	G to A	GAC	TGG	ATT	Trp to Stop
b5	94	G to C	GAA	GCT	GTG	Ala to Pro
b6	126	G to C	AGC	AGG	TGG	Arg to Ser
b7	214	C to T	GCG	CGA	CAA	Arg to Stop
b8[a]	34	C to T	CTA	CGA	ATC	Arg to Stop
b9	190–198	−GAC	GAC	GAC	GAC	Deletion
b10	106	G to T	GTT	GAT	AAG	Asp to Tyr
b11	113	C to A	AAG	TCG	CAG	Ser to Stop
b12	101	G to T	GTG	GGC	GTT	Gly to Val
b13	122	G to T	ATC	AGC	AGG	Ser to Ile
b14	196	G to T	GAC	GAC	ATG	Asp to Tyr
b15[a]	113	C to A	AAG	TCG	CAG	Ser to Stop
b16[a]	190–198	−GAC	GAC	GAC	GAC	Deletion
b17	34	C to T	CTA	CGA	ATC	Arg to Stop
b18	215	G to C	GCG	CGA	CAA	Arg to Pro
b19	113	C to T	AAG	TCG	CAG	Ser to Leu
b20	233	T to A	ATT	CTC	ACC	Leu to His
b21	104	T to G	GGC	GTT	GAT	Val to Gry
b22	42	G to T	ATC	GAG	AGT	Glu to Asp
b23	25	G to T	AAC	GAG	GCT	Glu to Stop
b24	117	G to T	TCG	CAG	ATC	Gln to His
b25	233	−T	ATT	CTC	ACC	Frameshift
b26	123	C to G	ATC	AGC	AGG	Ser to Arg
b27	169	G to C	GCT	GTT	CTT	Val to Leu
b28[a]	215	G to C	GCG	CGA	CAA	Arg to Pro
b29	155	C to T	TTC	TCA	ATG	Ser to Leu
b30	26	A to G	AAC	GAG	GCT	Glu to Gly
b31	34	C to T	CTA	CGA	ATC	Arg to Stop
b32	40	G to A	ATC	GAG	AGT	Glu to Lys
b33	117	G to T	TCG	CAG	ATC	Gln to His
b34	179–184	−G	TGG	GGG	GTC	Frameshift
b35	163	C to A	CTG	CTT	GCT	Leu to Ile
b36	150	G to T	CCA	AAG	TTC	Lys to Asn
b37	94	G to C	GAA	GCT	GTG	Ala to Pro
b38	221	T to C	CAA	GTT	GCT	Val to Ala
b39	73	G to A	CTT	GGA	ACT	Gly to Arg

[a] Ascribable to the same mutation obtained in an identical mouse.

the mutagenic activity by the following formula to compare the mutagenicity between azaPAHs:

fold-increase in *lacZ* MF (%) = *lacZ* MF obtained by test chemical/spontaneous *lacZ* MF × 100.
Mutagenic activity = fold-increase in *lacZ* MF/total dose of test chemical.

The organs given in capital letters in Table 12 indicate those that showed significant mutation and those given in small letters indicate negative organs. The underlined organs are those which showed the highest increase in *lacZ* MF. When the test chemical induced mutation in multiple organs, the mutagenic activity was calculated using the data of the underlined organs.

Although the five azaPAHs tested in our previous reports (quinoline, benzo[*f*]quinoline, benzo[*h*]quinoline, 1,7-phenanthroline and 10-azaBaP) induced mutation only in the specific organ such as the liver, 1,10-DAC and 4,10-DAC showed significant mutant frequencies in all of the six organs examined and the

Table 9
Sequences of *cII* mutations in the lung of control Muta™Mouse

Mutant no.	Position	Mutation	Sequence			Amino acid change
a1	146	C to T	ATT	CCA	AAG	Pro to Leu
a2	196	G to A	GAC	GAC	ATG	Asp to Asn
a3	113	C to T	AAG	TCG	CAG	Ser to Leu
a4	217	C to T	CGA	CAA	GTT	Gln to Stop
a5	180	G to A	GAA	TGG	GGG	Trp to Stop
a6	73	G to A	CTT	GGA	ACT	Gly to Arg
a7	132	G to T	TGG	AAG	AGG	Lys to Asn
a8	58–61	−A	AAC	AAA	ATC	Frameshift
a9	241–246	−A	AAA	AAA	CGC	Frameshift
a10	149–164	−AGTTCTCAATGCTGCT				Deletion
a11	25	G to T	AAC	GAG	GCT	Glu to Stop
a12	214	C to T	GCG	CGA	CAA	Arg to Stop
a13	197	A to G	GAC	GAC	ATG	Asp to Gly
a14	111	G to T	GAT	AAG	TCG	Lys to Asn
a15	206	G to C	GCT	CGA	TTG	Arg to Pro
a16	212	C to T	TTG	GCG	CGA	Ala to Val
a17	38	T to G	CGA	ATC	GAG	Ile to Ser
a18	40	G to A	ATC	GAG	AGT	Glu to Lys
a19[a]	40	G to A	ATC	GAG	AGT	Glu to Lys
a20	34	C to T	CTA	CGA	ATC	Arg to Stop
a21	90–91	GG to T	GCG	GAA	GCT	Frameshift
a22	113	C to T	AAG	TCG	CAG	Ser to Leu
a23	140	G to A	GAC	TGG	ATT	Trp to Stop
a24	110	A to T	GAT	AAG	TCG	Lys to Met
a25	175	G to A	CTT	GAA	TGG	Glu to Lys
a26	172	C to T	GTT	CTT	GAA	Leu to Phe
a27	89	C to T	ACA	GCG	GAA	Ala to Val
a28[a]	34	C to T	CTA	CGA	ATC	Arg to Stop
a29	221	T to G	CAA	GTT	GCT	Val to Gly
a30	273–275	ACA to CGATGCACG				Insertion
a31	212	C to T	TTG	GCG	CGA	Ala to Val
a32	193	G to A	GAC	GAC	GAC	Asp to Asn
a33	34	C to T	CTA	CGA	ATC	Arg to Stop
a34	31	C to G	GCT	CTA	CGA	Leu to Val
a35	155	C to A	TTC	TCA	ATG	Ser to Stop
a36	128	G to A	AGG	TGG	AAG	Trp to Stop
a37	88	G to T	ACA	GCG	GAA	Ala to Ser
a38[a]	34	C to T	CTA	CGA	ATC	Arg to Stop

[a] Ascribable to the same mutation obtained in an identical mouse.

highest *lacZ* mutant frequency in the lung. Chrysene also significantly induced mutation in all of the six organs examined, although chrysene showed similar mutant frequencies in all the six organs. These results suggest that nitrogen substitution in the chrysene skeleton may enhance the inducibility of mutation in the mouse lung.

4,10-DAC showed the highest mutagenic activity, followed in order by: quinoline > 1,7-phenenthroline ≈ 1,10-DAC > benzo[*h*]quinoline ≈ 10-azaBaP = benzo[*f*]quinoline. The number of mutagenic activity of chrysene is the same as that of benzo[*f*]quinoline, which shows the lowest mutagenic activity among the series of azaPAHs tested. The 4,10-DAC gave mutant frequencies higher than 1,10-DAC in all the test organs and the increase in *lacZ* MF obtained by 4,10-DAC is more than twice that by 1,10-DAC in most of the organs tested. Therefore, these results suggest that the nitrogen-substituted position affects the strength of mutagenicity of the DAC structure.

Table 10
Summary of *cII* mutation spectra in the liver of Muta™Mouse

Mutation class	Control (%)	1,10-DAC (%)	4,10-DAC (%)	Chrysene (%)
Total	30 (100)	38 (100)	38 (100)	36 (100)
Base substitution	26 (87)	35 (92)	35 (92)	32 (89)
Transitions				
GC to AT	14 (47)	7 (18)	8 (21)	9 (25)
AT to GC	1 (3)	2 (5)	0 (0)	2 (6)
Transversions				
AT to TA	1 (3)	3 (8)	1 (3)	2 (6)
AT to CG	2 (7)	1 (3)	1 (3)	1 (3)
GC to TA	7 (23)	17 (45)	18 (47)	13 (36)
GC to CG	1 (3)	5 (13)	7 (18)	5 (14)
−1 Frameshifts	2 (7)	1 (3)	1 (3)	3 (8)
+1 Frameshifts	0 (0)	0 (0)	0 (0)	0 (0)
Deletion	2 (7)	1 (3)	0 (0)	1 (3)
Insertion	0 (0)	0 (0)	0 (0)	0 (0)
Complex	0 (0)	1 (3)	2 (5)	0 (0)

The same mutations from an identical mouse were counted as a single event.

We further attempted *cII* mutant spectrum analysis in the liver and lung, which were shown to give the highest *lacZ* mutant frequencies by chrysene and DACs, respectively. In both organs, the spontaneous mutations consisted mainly of G:C to A:T transitions and the mutant spectrum in the control Muta™Mice showed no difference between the liver and lung. The G:C to A:T transitions in the control mice are likely to be ascribable to the deamination of 5-methylcytosine at the CpG site as previously reported [28]. DACs predominantly induced the G:C to T:A transversion in both organs. It was especially noteworthy that there was no difference in the *cII* mutant spectrum of 4,10-DAC between the lung and liver in spite of the quantitative difference showed by 4,10-DAC with its 3.9-fold higher *cII* mutant frequency in the lung than in the liver. These results suggest that the high mutagenicity in the lung of 4,10-DAC-treated mice might not arise from

Table 11
Summary of *cII* mutation spectra in the lung of Muta™Mouse

Mutation class	Control (%)	1,10-DAC (%)	4,10-DAC (%)	Chrysene (%)
Total	35 (100)	41 (100)	39 (100)	33 (100)
Base substitution	30 (86)	34 (83)	35 (90)	32 (91)
Transitions				
GC to AT	19 (54)	3 (7)	6 (15)	10 (29)
AT to GC	1 (3)	1 (2)	0 (0)	3 (9)
Transversions				
AT to TA	1 (3)	3 (7)	0 (0)	1 (3)
AT to CG	2 (6)	3 (7)	0 (0)	1 (3)
GC to TA	5 (14)	16 (39)	25 (64)	11 (31)
GC to CG	2 (6)	8 (20)	4 (10)	6 (17)
−1 Frameshifts	2 (6)	4 (10)	3 (8)	2 (6)
+1 Frameshifts	0 (0)	0 (0)	0 (0)	0 (0)
Deletion	1 (3)	0 (0)	0 (0)	1 (3)
Insertion	0 (0)	0 (0)	0 (0)	0 (0)
Complex	2 (6)	3 (7)	1 (3)	0 (0)

The same mutations from an identical mouse were counted as a single event.

Table 12
In vivo mutagenicity of a series of aza-PAHs

Chemical	Total dose (mg/kg)	Tested organ[a]							Mutagenic activity[b]		Sequence analysis	Ref.
Quinoline	250	LIVER	spleen	lung	kidney	bm	testis		1.76		Increase of GC to CG	[8–10]
Benzo[*f*]quinoline	400	LIVER	spleen	lung	kidney	bm			0.37		Featureless	[15]
Benzo[*h*]quinoline	400	liver	spleen	LUNG	kidney	bm			0.45		Featureless	[15]
1,7-Phenanthroline	200	LIVER	spleen	lung	kidney	bm			1.14		Increase of GC to CG	[15]
10-azaBaP	625	LIVER	spleen	lung	kidney	bm	COLON	gs fs	0.39		Featureless	[5]
1,10-DAC	400	LIVER	SPLEEN	LUNG	KIDNEY	BM	COLON		1.08		Increase of GC to TA	From this study
4,10-DAC	800	LIVER	SPLEEN	LUNG	KIDNEY	BM	COLON		2.32		Increase of GC to TA	From this study
Chrysene	800	LIVER	SPLEEN	LUNG	KIDNEY	BM	COLON		0.37		Increase of GC to TA	From this study

Superscript (c) in footnote (b) stands for fold-increase in *lacZ* MF (%) = *lacZ* MF obtained by test chemical/spontaneous *lacZ* MF × 100.
[a] The organs in capital letters are those that showed significant induction of mutation and those in small letters indicate negative organs. The underlined organ showed the highest increase in *lacZ* MF. BM(bm), bone marrow; gs, glandular stomach; fs, forestomach.
[b] Mutagenic activity = fold-increase in *lacZ* MF[c]/total dose of test chemical.

the increase of organ-specific adduct(s). In our previous studies, quinoline and 1,7-phenenthroline induced the G:C to C:G transversion [9]. On the other hand, 1,10-DAC and 4,10-DAC induced the G:C to T:A transversion. These results suggest that the enlargement of the molecular size in azaPAHs might change the major mutation pattern from the G:C to C:G transversion to the G:C to T:A transversion. Chrysene also increased the G:C to T:A transversion like DACs. Therefore, it was suggested that the nitrogen substitution in the chrysene skeleton may give no influence on the mutation spectrum.

We have previously reported that quinoline, a partial structure of DACs and one of simplest azaPAHs, showed mutagenicity in both in vitro [14,29] and in vivo [8] and that metabolic activation of quinoline might take place in the pyridine moiety to form the ultimate genotoxic form, an enamine epoxide (1,4-hydrated 2,3-epoxide) [10–14]. Moreover, benzo[*h*]quinoline and 1,7-phenanthroline, tricyclic azaPAHs with the quinoline moiety as a partial structure, may be activated in the pyridine moiety to show the mutagenicity as reported in our previous paper [16]. DACs, which consist of two quinoline moieties as a partial structure, might be also converted to the enamine epoxide structure in the pyridine moiety to be able to induce mutation. We are trying to investigate further to clarity the metabolic activation pathway of DACs.

In conclusion, it is suggested that the two types of nitrogen substitution in the chrysene structure enhances the mutagenicity in the mouse lung, although they have no influence on the organ specificity and mutation spectrum.

Acknowledgements

We thank Dr. T. Nohmi for his kind gift of *E. coli*, NM759 and BHB2688 and Dr. K. Masumura for his technical direction in making packaging extracts. This research is supported in part by the grant from Ministry of the Environment, Japan.

References

[1] Y. Kitahara, H. Okuda, K. Shudo, T. Okamoto, M. Nagao, Y. Seino, T. Sugimura, Synthesis and mutagenicity of 10-

azabenzo[*a*]pyrene-4,5-oxide and other pentacyclic aza-arene oxides, Chem. Pharm. Bull. 26 (1978) 1950–1953.
[2] C.H. Ho, B.R. Clark, M.R. Guerin, B.D. Barkenbus, T.K. Rao, J.L. Epler, Analytical and biological analysis of test materials from the synthetic fuel technologies, Mutat. Res. 85 (1981) 335–345.
[3] D.M. Jerina, R.E. Lehr, H. Yagi, O. Hernandez, P.M. Dansette, P.G. Wislocki, A.W. Wood, R.L. Chang, W. Levin, A.H. Conney, Mutagenicity of benzo[a]pyrene derivatives and the description of a quantum mechanical model which predict the ease of carbonium ion formation from diol epoxides, in: F.J. de Serres, J.R. Fouts, J.R. Bend, R.W. Philpot (Eds.), In vitro Metabolic Activation in Mutagenesis Testing, Elsevier-North Holland Biochem. Press, Amesterdam, 1976, pp. 159–177.
[4] A.W. Wood, R.L. Chang, W. Levin, D.E. Ryan, P.E. Thomas, H.D. Mah, J.M. Karle, H. Yagi, D.M. Jerina, A.H. Conney, Mutagenicity and tumorigenicity of phenanthrene and chrysene epoxides and diol epoxides, Cancer Res. 39 (1979) 4069–4077.
[5] K. Yamada, T. Suzuki, A. Kohara, M. Hayashi, A. Hakura, T. Mizutani, K. Saeki, Effect of 10-aza-substitution on benzo[*a*]pyrene mutagenicity in vivo and in vitro, Mutat. Res. 521 (2002) 187–200.
[6] K. Hirao, Y. Shinohara, H. Tsuda, S. Fukushima, M. Takahashi, Carcinogenic activity of quinoline on rat liver, Cancer Res. 36 (1976) 329.
[7] Y. Shinohara, T. Ogiso, M. Hananouchi, K. Nakanishi, T. yoshimura, N. Ito, Effect of various factors on the induction of liver tumors in animals by quinoline, Jpn. J. Cancer Res. 68 (1977) 785–796.
[8] T. Suzuki, Y. Miyata, K. Saeki, Y. Kawazoe, M. Hayashi, T. Sofuni, In vivo mutagenesis by the hepatocarcinogen quinoline in the *lacZ* transgenic mouse: evidence for its in vivo genotoxicity, Mutat. Res. 412 (1998) 161–166.
[9] T. Suzuki, X. Wang, Y. Miyata, K. Saeki, A. Kohara, Y. Kawazoe, M. Hayashi, T. Sofuni, Hepatocarcinogen quinoline induces G:C to C:G transversions in the *cII* gene in the liver of lambda/*lacZ* transgenic mice (MutaMouse), Mutat. Res. 456 (2000) 73–81.
[10] Y. Miyata, K. Saeki, Y. Kawazoe, M. Hayashi, T. Sofuni, T. Suzuki, Antimutagenic structure modification of quinoline assessed by an in vivo mutagenesis assay using *lacZ*-transgenic mice, Mutat. Res. 414 (1998) 165–169.
[11] M. Tada, K. Takahashi, Y. Kawazoe, N. Ito, Binding of quinoline to nucleic acid in a subcellular microsomal system, Chem. Biol. Interact. 29 (1980) 257–266.
[12] M. Tada, K. Takahashi, Y. Kawazoe, Metabolites of quinoline, a hepatocarcinogen, in a subcellular microsomal system, Chem. Pharm. Bull. 30 (1982) 3834–3837.
[13] K. Takahashi, M. Kamiya, Y. Sengoku, K. Kohda, Y. Kawazoe, Deprivation of the mutagenic property of quinoline: inhibition of mutagenic metabolism by fluorine substitution, Chem. Pharm. Bull. 36 (1988) 4630–4633.
[14] K. Saeki, K. Takahashi, Y. Kawazoe, Metabolism of mutagenicity-deprived 3-fluoroquinoline: comparison with mutagenic quinoline, Biol. Pharm. Bull. 16 (1993) 232–234.
[15] K. Yamada, T. Suzuki, A. Kohara, M. Hayashi, T. Mizutani, K. Saeki, In vivo mutagenicity of benzo[*f*]quinoline, benzo[*h*]quinoline, and 1,7-phenanthroline using the *lacZ* transgenic mice, Mutat. Res. 559 (2004) 83–95.
[16] K. Saeki, H. Kawai, Y. Kawazoe, A. Hakura, Dual stimulatory and inhibitory effects of fluorine-substitution on mutagenicity: an extension of the enamine epoxide theory for activation of the quinoline nucleus, Biol. Pharm. Bull. 20 (1997) 646–650.
[17] K. Yamada, A. Hakura, T. Kato, T. Mizutani, K. Saeki, Nitrogen substitution effects on the mutagenicity and cytochrome P450 isoform-selectivity of chrysene analogs, Mutat. Res., in press.
[18] S.V. Nekrasov, A.V. El'tsov, Polynuclear aza-aromatic compounds, I. Zh. Org. Khim. 7 (1971) 188–199.
[19] W.C. Summers, P.M. Glazer, D. Malkevich, Lambda phage shuttle vectors for analysis of mutations in mammalian cells in culture and in transgenic mice, Mutat. Res. 220 (1989) 263–268.
[20] E.J. Gunther, N.E. Murray, P.M. Glazer, High efficiency, restriction-deficient in vitro packaging extracts for bacteriophage lambda DNA using a new *E.coli* lysogen, Nucleic Acids Res. 21 (1993) 3903–3904.
[21] J.A. Gossen, A.C. Molijn, G.R. Douglas, J. Vijg, Application of galactose-sensitive *E. coli* strains as selective hosts for *LacZ*-plasmids, Nucleic Acids Res. 20 (1992) 3254.
[22] S.W. Dean, B. Myhr, Measurement of gene mutation in vivo using Muta Mouse and positive selection for *lacZ*-phage, Mutagenesis 9 (1994) 183–185.
[23] J. Jiao, G.R. Douglas, J.D. Gingerich, L.M. Soper, Comparison of the molecular characteristics of *lacZ* transgenic mouse mutations detected by visual and positive selection, Mutat. Res. 372 (1996) 141–145.
[24] J.L. Jakubczak, G. Merlino, J.E. French, W.J. Muller, B. Paul, S. Adhya, S. Garges, Analysis of genetic instability during mammary tumor progression using a novel selection-based assay for in vivo mutations in a bacteriophage lambda transgene target, Proc. Natl. Acad. Sci. U.S.A. 93 (1996) 9073–9078.
[25] Collaborative Study Group on the Transgenic Mutation assay (CSGTM), Organ variation in the mutagenicity of ethylnitrosourea in Muta mouse: results of the collaborative study on the transgenic mutation assay by JEMS/MMS, Environ. Mol. Mutagen., 28 (1996) 363–375.
[26] H. Ikehata, M. Takatsu, Y. Saito, T. Ono, Distribution of spontaneous CpG-associated G:C → A:T mutations in the lacZ gene of Muta mice: effects of CpG methylation, the sequence context of CpG sites, and severity of mutations on the activity of the *lacZ* gene product, Environ. Mol. Mutagen. 36 (2000) 301–311.
[27] T. Suzuki, An evaluation of the transgenic mouse mutation assays, Environ. Mutagen. Res. 25 (2003) 119–125.
[28] R. Holliday, G.W. Grigg, DNA methylation and mutation, Mutat. Res. 285 (1993) 61–67.
[29] T. Kato, K. Saeki, Y. Kawazoe, A. Hakura, Effects of oligofluorine substitution on the mutagenicity of quinoline: a study with twelve fluoroquinoline derivatives, Mutat. Res. 439 (1999) 149–157.

New Approaches to Mechanism Analysis for Drug Discovery Using DNA Microarray Data Combined with ***KeyMolnet***

Hiromi Sato[1]*, Seiichi Ishida[2], Kyoko Toda[2], Rieko Matsuda[2], Yuzuru Hayashi[2], Makoto Shigetaka[1], Miki Fukuda[1], Yohko Wakamatsu[1] and Akiko Itai[1]

[1] *Institute of Medicinal Molecular Design, Inc. (IMMD), 5-24-5 Hongo, Bunkyo-ku, Tokyo 113-0033, Japan*

[2] *National Institute of Health Sciences, 1-18-1 Kami-Yoga, Setagaya, Tokyo 158-8501, Japan*

Abstract: We have developed a comprehensive information platform, named KeyMolnet, for drug discovery and life science research in the post-genome era. Using KeyMolnet, we show new approaches to research into the biological mechanism in DNA microarray analysis. Thanks to the DNA microarray technology, it is now possible to obtain very large quantities of gene expression data at a time. However, it is still difficult to extract meaningful information from such large quantities of data and to analyze the relationship between gene expression data and biological function. We therefore developed an advanced tool that can generate molecular networks upon demand, and beyond signaling "cross-talks," can connect them to physiological phenomena and medical and drug information. Here we show the methods of mechanism analysis using the DNA microarray data and KeyMolnet, as well as the possible mechanism of inducing apoptosis in the human promyelocytic leukemia cell line, HL-60, treated with 12-*O*-tetradecanoylphorbol 13-acetate (TPA), using the time series of gene expression data from DNA microarray experiments. KeyMolnet enables practical approaches to research into biological mechanisms, which in turn contribute to new discoveries in the medical, pharmaceutical and life sciences.

Keywords: DNA microarray, proteomics, network, molecular relation, data mining, platform, apoptosis.

INTRODUCTION

DNA microarray analysis has been actively performed to discover new clinical markers, establish prognostic expectations, create tailor-made medications, discover new drugs, etc. in recent years. We can now obtain large quantities of gene expression data at a time, thanks to this new technology. R&D in the medical, pharmaceutical and life sciences is making great progress by using gene expression profiles effectively. In fact, Alizadeh *et al.* achieved significant results with prognostic implications that had not been expected before, and identified distinct types of diffuse, large B-cell lymphoma by gene expression profiling using DNA microarray technology [1]. Differential gene expression classification of the most common subtype of non-Hodgkin's lymphoma is clinically useful, however, the biological significance has not been clear with the gene expression classification alone so far. Tools for cluster analysis and display systems for DNA microarray data are already available, but they are not yet adequate for deriving biological functions from comprehensive gene expression data. Protein-protein interaction networks are needed to provide biological functions. A platform and an application for extracting significant data from large quantities of available data, for generating networks based on the data, and furthermore, for clarifying the biological functions based on the networks and/or connecting networks, have long been awaited.

*Address correspondence to this author at the Institute of Medicinal Molecular Design, Inc. (IMMD), 5-24-5 Hongo, Bunkyo-ku, Tokyo 113-0033, Japan; Tel: +81-3-5689-4052; Fax: +81-3-5689-4054; E-mail: hiromis@immd.co.jp

Even with a goldmine of information on genes and proteins, it would still be difficult to clarify their biological functions and biological phenomena without such a system.

For this reason we have developed the definitive mining tool, KeyMolnet, which can generate networks from any molecules and can connect the networks to biological phenomena, and drug and disease information.

The KeyMolnet system consists of a "content database" and "search software." The content database stores pairs of molecules, e.g. proteins and small molecules, based on their relational information from the literature, review articles and papers. From pairs of molecules in the content database, networks can be generated upon demand, in real time, by the search software. The content database stores information on diseases and drugs besides the information on molecules and molecular relations. All the information on molecules, molecular relations, diseases and drugs is carefully curated and manually collected by the researchers at the Institute of Medicinal Molecular Design, Inc. (IMMD). Furthermore, hundreds of canonical pathways including "signal transduction pathways," "metabolic pathways" and "transcriptional regulations" are also manually compiled. The content database also stores information from publicly available databases such as Swiss Prot [2] and Gene Ontology (GO) [3]. The client application performs various search functions by combining mainly three searching methods and some logical operations. The three searching methods are "Keyword search," "Related item search" and "Network search." "Related item search" involves information on the relationships between molecules and other items such as diseases, drugs and GO. "Network

1570-1638/05 $50.00+.00

search" involves the following relationships between molecules in appropriate ways depending on users' search conditions. "Network search" is based on graph theory.

Users can analyze experimental data such as DNA microarray and proteomics by importing the data into KeyMolnet, and can also add the original information and/or public data.

Furthermore, KeyMolnet also provides logical operation functions such as AND, OR and DIFF (meaning "subtraction") operation functions. Using these functions, users can extract intersectional and/or difference networks for several datasets under different experimental conditions.

In this way, the networks and pathways derived from gene expression data can be shown, and mechanisms can be suggested by connecting the generated networks with information on biological phenomena, diseases and drugs, mediated by molecules common to them in KeyMolnet.

It is well known that the human promyelocytic leukemia cell line, HL-60 can be induced to differentiate into macrophage-like cells by 12-*O*-tetradecanoylphorbol 13-acetate (TPA) [4]. TPA is a potent tumor promoter and can convert human promyelocytic leukemia cells into nonproliferating cells with many characteristics of macrophages [5, 6]. It is also known that TPA induces apoptosis of the cell line during differentiation [7]. However, so far further details on the mechanism of apoptosis induction have been unclear, even that in the cells. Here we show a possible mechanism for the pathway based on data from the up-regulated genes obtained by DNA microarray analysis to the induction of apoptosis in the TPA-treated cells.

With the KeyMolnet client application, users can search information in the content database, view the search results interactively, compare and evaluate the search results. Furthermore, users can also search and/or view while interactively adding their original information such as hypothetical and/or experimental data.

MATERIALS AND METHODS

KeyMolnet system is available from the Institute of Medicinal Molecular Design, Inc. (IMMD) [8, http://www.immd.co.jp].

Content Database

The tables of the content database fall into the following five main categories: "Molecule Information Table," "Molecular Relation Table," "Disease Information Table," "Drug Information Table" and "GO Table." The "Molecule Information Table" stores information on individual molecules such as molecule IDs (referred to as "KeyMolnet IDs"), molecule symbols, synonyms, comments and other annotation data items. A "Molecule" is given as a node with a unique "KeyMolnet ID" in an abbreviated form and is represented as oval, rectangular, capsule-like and hexagonal shapes, indicating proteins, small molecules, complexes and exogenous molecules, respectively, on networks. The "Molecular Relation Table" stores information on pairs of molecules and additional data on the molecular relations such as "Direct," "Indirect," "Transcriptional Regulation," "Positive" and/or "Negative," and additional annotation data items. When several molecules form a complex and the complex reacts with other molecules, the relation between the complex and its component molecules is described as "Complex-Member" in KeyMolnet. The types of "Molecular Relations" are represented by different kinds of edges, arrows and colors in figures. The "Disease Information Table" stores extensive information on molecules (referred to as "Mediating Molecules") involved in the onset and/or development of a certain disease, and on the symptoms, signs, and causes of the disease and/or the results of changes in the "Mediating Molecule" in the disease state (referred to as "Pathological Event"). Furthermore, information on the relation between the "Mediating Molecule" and the "Pathological Event" is included in the "Disease Information Table." The "Drug Information Table" stores the "Drug Molecule" of all FDA-approved drugs and their "Target Molecule" that is quantitatively and/or qualitatively subjected to the action of specific drugs. The "GO Table" stores information on GO terms involved in the "Biological Process" of the GO of molecules that correspond to their Swiss Prot IDs using GO Annotation (GOA) [9]. In KeyMolnet, "Molecules" are basically defined as proteins and small molecules. Therefore, a network in KeyMolnet is given as a "protein network", is not as a "gene network." All information on molecules, molecular relations, diseases and drugs was manually collected and carefully curated by the IMMD researchers.

Search Software

System Architecture

KeyMolnet is implemented as a server-client system. The content database is managed by the relational database management system (RDBMS) and the client application is written in the C++ language and runs on a Windows platform.

Search Method

The KeyMolnet client application performs various search functions by combining mainly three searching methods and three logical operations. The three searching methods are "Keyword search," "Related item search" and "Network search." "Related item search" is performed on information on the relations between molecules and other items such as diseases or GO. Furthermore, canonical pathways such as the "Ras signaling pathway" and the "TCA cycle" can be called up from the pathway list by the "Pathway search," because the canonical pathways are also stored and manually compiled based on the pairs of molecules in the content database. "Network search" is performed by the following relationships between molecules in appropriate ways depending on users' search conditions. "Network search" is based on graph theory.

Network Search Method

The following three patterns of network search method are provided: "Neighboring search method," "N-points to N-points search method" and "Common upstream/downstream